Benchmark 19 calculated with milonga

Camusso, C.P.

August 16, 2016

Contents

List of Figures

List of Tables

1 Codes used

1. The codes used were:

   milonga 0.4.65 (45d6523484f3 2016-07-02 10:45 -0300) [2]

   free nuclear reactor core analysis code

   rev hash 45d6523484f38dcce25bb1f52779a6ff620a5eb8

   last commit on 2016-07-02 10:45 -0300 (rev 287)

   compiled on 2016-07-02 21:27:52 by pablo@pablo (linux-gnu x86_64)

   with gcc (Debian 4.9.2-10) 4.9.2 using -O2 linked against

SLEPc Release Version 3.6.2, Nov 03, 2015

Petsc Release Version 3.6.3, Dec, 03, 2015 arch-linux2-c-debug

running on Linux 3.16.0-4-amd64 #1 SMP Debian 3.16.7-ckt25-2 (2016-04-08) x86_64

2 Intel(R) Core(TM)2 CPU 6300 @ 1.86GHz

milonga is copyright (c) 2010-2015 jeremy theler

licensed under GNU GPL version 3 or later.

milonga is free software: you are free to change and redistribute it.

There is NO WARRANTY, to the extent permitted by law.

——– ——- ——- —– —- —-

wasora 0.4.117 (14dccdd2711f+ 2016-07-18 11:38 -0300) [3]

wasora's an advanced suite for optimization & reactor analysis

rev hash 14dccdd2711f7eea767f5b6a01aa509235e385e4

last commit on 2016-07-18 11:38 -0300 (rev 272)

compiled on 2016-07-18 21:01:48 by pablo@pablo (linux-gnu x86_64)

with gcc (Debian 4.9.2-10) 4.9.2 using -O2 and linked against

GNU Scientific Library version 1.16

SUNDIALs Library version 2.5.0

GNU Readline version 6.3

wasora is copyright (C) 2009-2016 jeremy theler

licensed under GNU GPL version 3 or later.

wasora is free software: you are free to change and redistribute it.

There is NO WARRANTY, to the extent permitted by law.

and ——————————————————————————

Petsc Release Version 3.5.2, Sep, 08, 2014

The PETSc Team

petsc-maint@mcs.anl.gov

http://www.mcs.anl.gov/petsc/

See docs/changes/index.html for recent updates.

See docs/faq.html for problems.

See docs/manualpages/index.html for help.

Libraries linked from /home/geuzaine/src/petsc-3.5.2/linux_complex_mumps_seq/lib

——————————————————————————

2.12.0 [4]

2 Introduction

1. The benchmark ANL-7416-19 [5] was calculated using the milonga code.
2. This benchmark is about a 2D PWR with depletion and fuel management.
3. The function of this benchmark is is to provide a test for the capabilities of coarse mesh methods for PWR fuel management calculations.
4. The loading pattern of the first cycle is shown in the Figure 1.

5. The refueling pattern of the second cycle is shown in the Figure 2.

6. The control rod configuration is shown in the Figure 3.

7. Note: The assembly which is moved from its cycle 1 position (I,J)=(8,2) to positions (5,1) and (7,1) at the main axis is to be symmetrized, at reload time and after rotating it as shown in the Figure 2, according to the following rule

$$P_{sym}(x,y) = \frac{1}{2}\left[P(x,y) + P(x,-y)\right], \tag{1}$$

with

$$0 \leq y \leq \frac{H}{2}, \tag{2}$$

where $P(x,y)$ denotes the local burnup and the local nuclide number densities, respectively.

8. Details:

   8.1 The problem is set up to allow the use of computer codes which model either a quarter core or a reactor octant.

   8.2 Vacuum boundary conditions at external boundaries, reflective boundary conditions at symmetry lines.

   8.3 Homogeneus reflector.

   8.4 Specified nuclide depletion chains (Figure 4)

      8.4.1 initial nuclide densities,

      8.4.2 microscopic cross sections of burnable nuclides,

      8.4.3 macroscopic cross sections of structural materials.

   8.5 Reactor is maintained critical throughout life by adjusting the amount of soluble boron (measured in ppm).

   8.6 The cycle length is defined by requiring the critical boron concentration to become equal to zero.

   8.7 The selection of time steps is not specified. The benchmark problem solution should approximate as closely as possible the case of infinitely small time steps.

   8.8 Burnable poison is present in some of the assemblies of types E2 and E3, where indicated in the loading pattern of first cycle, Figure 1.

   8.9 At EOC1 the burnable poison is not set to zero but moves with the assemblies at BOC2. All fresh assemblies loaded at the beginning of the second cycle are of type E3 and contain no burnable poison, Figure 2.

   8.10 Control rods are described by adding spatially constant macroscopic cross sections to the respective cross sections of the structural material of the unrodded assemblies.

   8.11 The soluable boron and structural material are not to be depleted.

   8.12 The isotopic depletion equations for nuclides 1 to 8 are:

$$\frac{dN_j}{dt} + \left[\sum_g \sigma_{aj}^g \Phi_g + \lambda_j\right] N_j = N_{j-1} \sum_g \sigma_{cj-1}^g \Phi_g \tag{3}$$

   Note: For nuclides j=3 (U238) and j=8 (burnable poison BP) the source term is 0.

   8.13 For nuclide j=9 (Xe135) the equilibrium concentration is to be determined by:

$$N_{Xe}^{\infty} = \frac{\sum_j \gamma_{Xe}^j N_j \sum_g \sigma_{fj}^g \Phi_g}{\sum_g \sigma_{cXe}^g \Phi_g + \lambda_{Xe}} \tag{4}$$

Figure 1: Loading pattern of first cycle

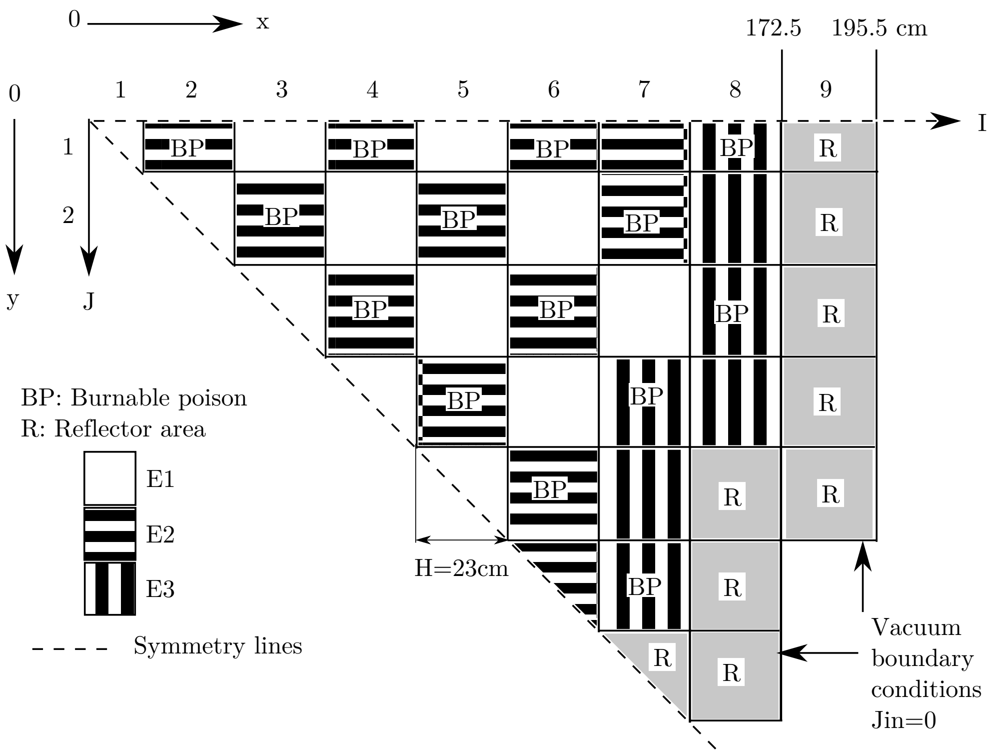

Figure 2: Refueling pattern of second cycle

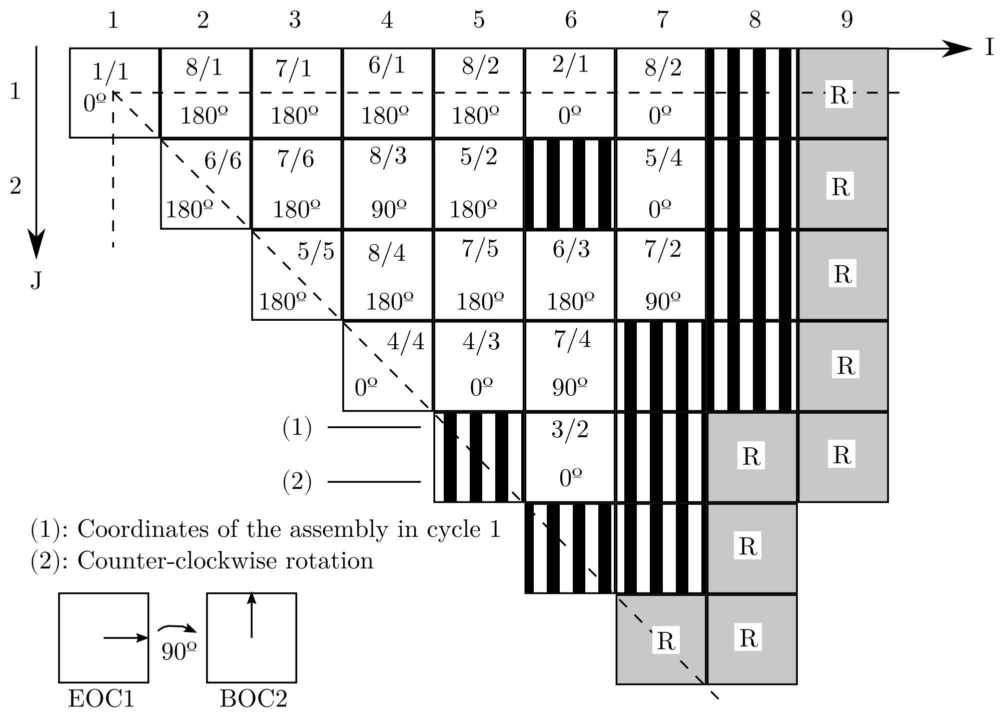

Assemblies loaded into a position at a symmetry line are symmetrized according to the symmetry at their new position.

Figure 3: Control rod configuration

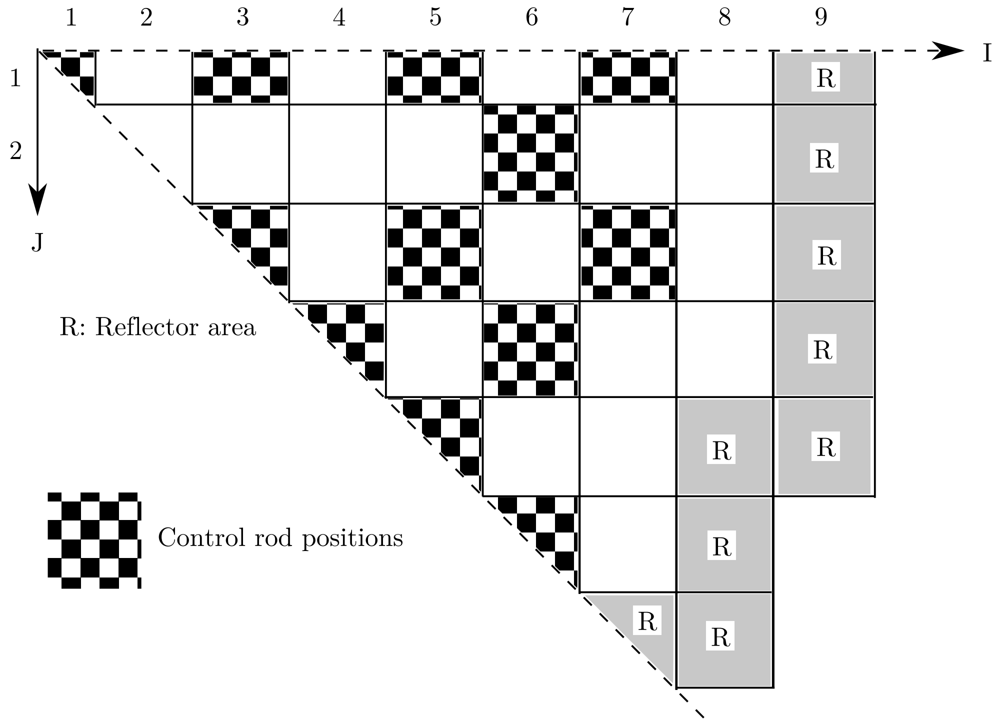

Figure 4: Nuclide depletion chains

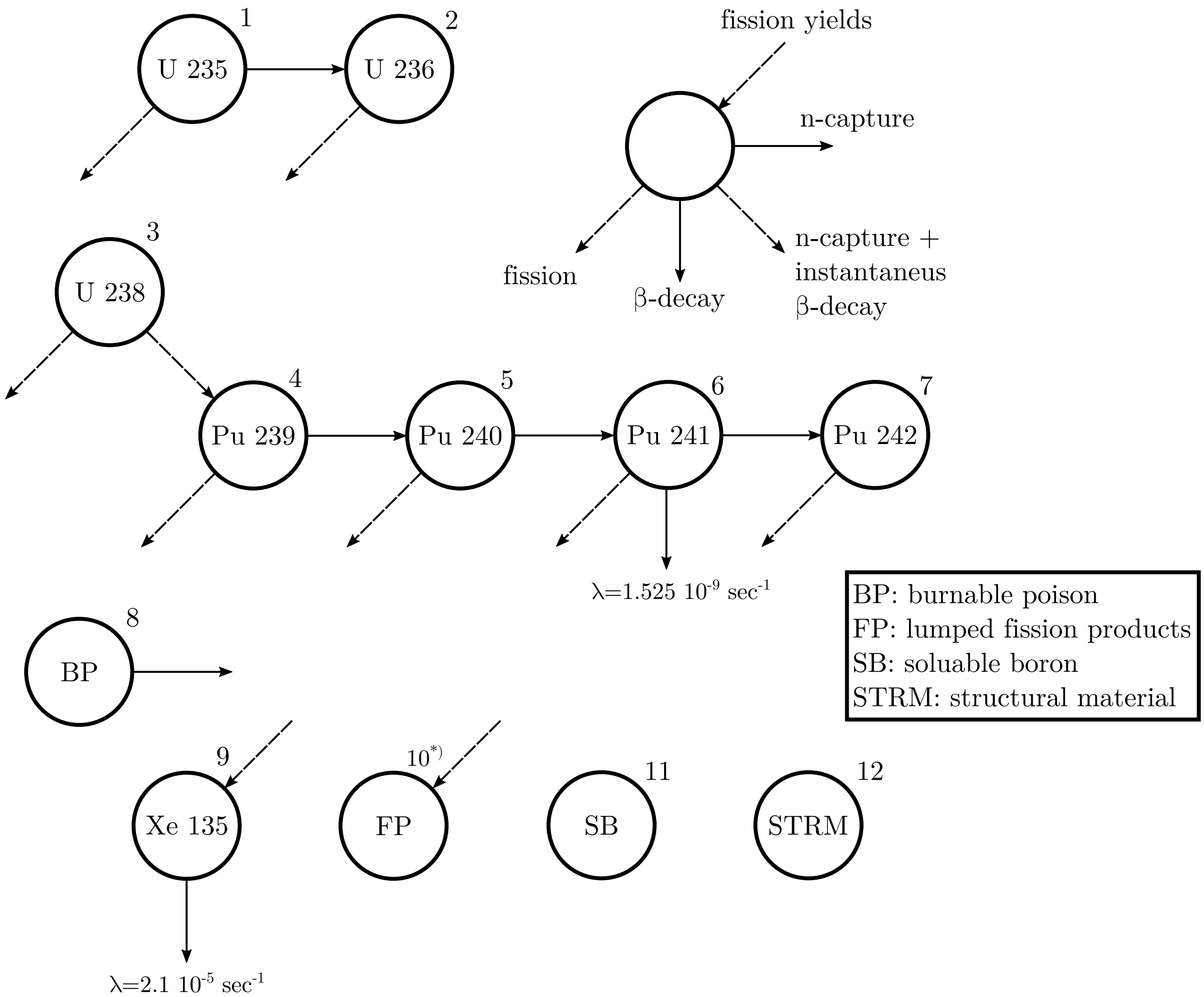

Table 1: Initial nuclide densities (units of 10^{24} atoms/cm^3)

Nuclide	Fuel assembly type		
	E1	E2	E3
U235	1.40 10^{-4}	1.60 10^{-4}	2.20 10^{-4}
U238	6.31 10^{-3}	6.29 10^{-3}	6.23 10^{-3}
BP	0	8.00 10^{-6} [a)]	8.00 10^{-6} [a)]

All other depletable nuclides have zero initial number densities.

[a)] where present according to the load pattern of cycle 1, Figure 1.

8.14 The depletion equation of the fission products (FP) j=10 has no loss term:

$$\frac{dN_{FP}}{dt} = \sum_{j=1}^{7} \gamma_{FP}^{j} N_j \sum_g \sigma_{fj}^{g} \Phi_g \tag{5}$$

9. The Table 1 shows the initial nuclide densities (units of 10^{24} atoms/cm^3).

10. Reduction of source situation

10.1 Diffusion theory.

10.2 Two energy groups.

10.3 Zero axial leakage.

10.4 Reactor is maintained critical at all times by adjusting the amount (ppm) of soluble boron (except fot the rodded reactor at EOC1, see item 107 below).

10.5 The reactor is at all times in its (instantaneous) xenon equilibrium state.

10.6 In addition, the critical state of the xenon-free reactor is to be determined at BOC1, EOC1, and BOC2 (see below).

10.7 The control rods are withdrawn during depletion. At the beginning of cycles 1 and 2 the following procedure should be followed for determining the rod worth and the power distribution for the unrodded reactor:

10.7.1 Compute the critical boron concentration c^0_{BOC} (unrodded) for the unrodded, xenon-free reactor.

10.7.2 Insert the control rods and compute the critical boron concentration c^0_{BOC} (rodded) and the normalized power distribution for the rodded, xenon-free core.

10.8 At end of cycle 1 the procedure is

10.8.1 Compute c^0_{EOC} (unrodded) for the xenon-free, unrodded reactor.

10.8.2 Keep the soluable boron fixed at c^0_{EOC} (unrodded) and compute the reactivity of the rodded, xenon-free reactor.

10.9 The non-linear two-group diffusion equations to be solved are

$$-\nabla D^1 \nabla \Phi_1 + \Sigma_r^1 \Phi_1 = \sum_j N_j \sum_g \nu_j^g \sigma_{fj}^g \Phi_g, \tag{6}$$

$$-\nabla D^2 \nabla \Phi_2 + \Sigma_r^2 \Phi_2 = \Sigma^{12} \Phi_1. \tag{7}$$

where ppm is the eigenvalue (with the exception of the rodded reactor at EOC1 where k_{eff} is the eigenvalue) and the following cross sections definitions apply:

$$\Sigma_r^1 = \Sigma^{12} + \Sigma_c^1 + \Sigma_f^1 + ppm \cdot \sigma_{c,SB}^1 \tag{8}$$

$$\Sigma_r^2 = \Sigma_c^2 + \Sigma_f^2 + ppm \cdot \sigma_{c,SB}^2 + \sigma_{c,Xe}^2 N_{Xe}^{\infty} \tag{9}$$

$$D^g = \frac{1}{3\Sigma_{tr}^g}. \tag{10}$$

Note: The macroscopic cross sections Σ^g include contributions from the structural material Σ_{STRM}. For the rodded reactor there are additional contributions $\Delta\Sigma_R$ from the control rods for all rodded assemblies of Figure 3. These contributions are indicated by brackets.

10.10 Transport cross sections:

$$\Sigma_{tr}^g = \Sigma_{tr,STRM}^g \tag{11}$$

10.11 Fission:

$$\Sigma_f^g = \sum_{j=1}^{7} \sigma_{fj}^g N_j \tag{12}$$

10.12 Capture (not including soluable boron and xenon):

$$\Sigma_c^g = \sum_{j \neq 9,11} \sigma_{cj}^g N_j + \Sigma_{c,STRM}^g + (\Delta\Sigma_{c,R}^g) \tag{13}$$

10.13 Slowing down:

$$\Sigma^{12} = \Sigma_{STRM}^{12} + (\Delta\Sigma_R^{12}) \tag{14}$$

10.14 The two-group cross sections and other data are listed in the following tables:

10.14.1 Table 2: Microscopic cross sections of fissionable nuclides.

10.14.2 Table 3: Microscopic cross sections of nuclides 8 to 11.

10.14.3 Table 4: Fission product yields.

10.14.4 Table 5: Macroscopic cross sections of the structural material.

10.14.5 Table 6: Macroscopic cross sections of the control rods.

11. Additional data:

11.1 Average power density is 93 Watt/cm^3 at all times (averaged over entire octant core) resp. 1.186877625 10^6 Watt/cm for the reactor octant.

11.2 The burnup (exposure) is expressed in units of MWD/kgU.

11.3 The uranium mass density in all assembly types is 2.54 10^{-3} kg/cm^3.

3 Expected results

1. For reactor cycles 1 and 2:

1.1 Critical boron concentration (ppm) at discrete time points.

1.2 Average normalized assembly powers at BOC and EOC.

1.3 Average assembly burnups at EOC.

1.4 Average nuclide densities for each fuel batch at EOC.

1.5 Cycle length in unis of full power days (FPD).

1.6 Critical boron concentration and normalized power distribution for the rodded, xenon-free reactor (BOC1 and BOC2).

1.7 Reactivity of the rodded, xenon-free reactor (EOC1).

1.8 Total running time and computer used.

1.9 The benchmark also suggest additional results; but they were not calculated.

Table 2: Microscopic cross sections of fissionable nuclides (unit $10^{-24}cm^2$)

Nuclide	Group	Assembly type						Neutrons per fission
		E1		E2		E3		
j	g	σ_f^g	σ_c^g	σ_f^g	σ_c^g	σ_f^g	σ_c^g	ν_j^g
1 U235	1	7.60	4.20	7.50	4.10	7.40	4.00	2.44
	2	238.60	42.90	231.90	41.80	220.60	39.80	2.44
2 U236	1	0.20	7.90	0.20	7.80	0.20	7.70	2.79
	2	0.00	2.70	0.00	2.70	0.00	2.60	0.00
3 U238	1	0.12	0.85	0.12	0.84	0.12	0.84	2.85
	2	0.00	1.23	0.00	1.20	0.00	1.15	0.00
4 Pu239	1	9.80	6.40	9.70	6.40	9.70	6.40	2.90
	2	617.00	348.10	611.60	347.00	601.50	344.50	2.88
5 Pu240	1	0.60	10.00	0.60	10.00	0.60	10.00	3.10
	2	0.10	915.90	0.10	977.50	0.10	1081.20	2.89
6 Pu241	1	18.50	4.70	18.40	4.70	18.20	4.70	3.02
	2	635.20	222.80	622.30	218.90	599.90	212.00	2.94
7 Pu242	1	0.50	36.50	0.50	36.20	0.50	35.70	3.11
	2	0.00	9.90	0.00	9.80	0.00	9.50	0.00

χ_j^g, the energy released per fission event is $\chi_j^g = 0.32\ 10^{-10} W$ for all fisionable nuclides j, groups g and assembly types.

Table 3: Microscopic cross sections σ_c of nuclides 8 to 11 (units $10^{-24}cm^2$ for nuclides 8-10, unit $cm^{-1}ppm^{-1}$ for nuclide 11.)

Nuclide	Group	σ_c^g (All assembly types)
j	g	
8 BP	1	28.00
	2	800.0
9 Xe135	1	0.0
	2	$1.20\ 10^6$
10 FP	1	5.3
	2	36.5
11 SB*)	1	$1.40\ 10^{-7}$
	2	$9.38\ 10^{-6}$

*) Note: units for nuclide 11 are $cm^{-1}ppm^{-1}$.

Table 4: Fission product yields γ_k^j (all assembly types)

Nuclide	U235	U236	U238	Pu239	Pu240	Pu241	Pu242
k\j	1	2	3	4	5	6	7
9 Xe135	0.0663	0.0665	0.0665	0.0747	0.0665	0.0708	0.0665
10 FP	1.0	1.0	1.0	1.0	1.0	1.0	1.0

Table 5: Macroscopic cross sections (cm^{-1}) of the structural material STRM. Note: $D_g = 1/(3\Sigma_{tr}^g)$

Assembly type	Group	$\Sigma_{c,STRM}^g$	$\Sigma_{tr,STRM}^g$	Σ_{STRM}^{12}
E1	1	$6.51\ 10^{-4}$	0.222	$1.89\ 10^{-2}$
	2	$7.02\ 10^{-3}$	0.835	
E2	1	$6.50\ 10^{-4}$	0.222	$1.88\ 10^{-2}$
	2	$6.93\ 10^{-3}$	0.829	
E3	1	$6.50\ 10^{-4}$	0.222	$1.85\ 10^{-2}$
	2	$6.78\ 10^{-3}$	0.820	
Reflector	1	$9.80\ 10^{-4}$	0.257	$2.37\ 10^{-2}$
	2	0.138	1.31	

Table 6: Macroscopic cross section of the control rods, all assembly types

Group g	$\Delta\Sigma_{c,R}^g$	$\Delta\Sigma_R^{12}$
1	0.002	-0.003
2	0.020	-

4 References

[1] FDL licence. https://www.gnu.org/licenses/fdl-1.2-standalone.html

[2] Milonga code. https://bitbucket.org/wasora/milonga/overview

[3] Wasora code. https://bitbucket.org/wasora/wasora

[4] gmsh: mesh generator. http://gmsh.info/

[5] ANL-7416-19. http://www.corephysics.com/benchmarks/anl7416_benchmark19.pdf